

Analysis of Guided Wave Structures Using 3-D Envelope-Finite Element (EVFE) Technique

Hsiao-Ping Tsai, Yuanxun Wang, and Tatsuo Itoh

Electrical Engineering Department, University of California, Los Angeles
405 Hilgard Avenue, Los Angeles, CA 90095

Abstract — A novel three-dimensional Envelope-Finite Element (EVFE) technique is proposed to solve the transient response of an electromagnetics problem. EVFE simulates the signal envelope rather than the original signal waveform by de-embedding the signal carrier from the time-domain wave equation. The sampling rate of the time-domain waveform is only governed by the Nyquist rate of the envelope signal instead of the carrier signal in the unconditionally stable FETD method. Compared to the traditional FDTD and FETD methods, the computational cost can be dramatically reduced when the signal envelope and carrier ratio is very small. This technique is implemented to solve a microwave guided structure with dielectric post discontinuity. The accuracy and efficiency is demonstrated and compared with the unconditionally stable FETD method.

I. INTRODUCTION

Recently, with the rapid development of powerful computers with large memory capacities, the direct solution methods of differential form wave equations in the time domain have been introduced. By using time domain analysis, the transient response and the wideband frequency information can be obtained in one single simulation. The finite difference time domain (FDTD) technique is one of the most extensively used methods due to its numerical efficiency and simplicity in formulation and implementation [1]. However, the FDTD analysis has difficulty in dealing with geometrically irregular structures. Many techniques have been proposed to overcome this difficulty and to provide efficient yet accurate algorithms. One of these techniques is the edge-based finite element time domain (FETD) method. The mesh flexibility of the FETD method allows geometrically complex structures and circuits containing inhomogeneous, anisotropic, or even nonlinear materials. Gedney *et al.* [2] proposed an unconditionally stable FETD solution based on the second-order electric field Maxwell's equation. The time-dependent formulation employs a time-integration method based on the Newmark-Beta method. With appropriate values of the parameters controlling the accuracy and the stability of the scheme, the Newmark method yields an unconditionally stable scheme with second-order accuracy. This algorithm

has been extended as Unconditionally Stable Extended (USE) FETD method [3] to incorporate a nonlinear microwave amplifier into the FETD method. The result has shown that this scheme reduces computation time over the conditionally stable FETD method by at least ten times. However, when the unconditionally stable FETD scheme is applied to solve a problem which has a much narrower signal bandwidth than the carrier frequency, the time step is still constrained by the maximum operating frequency, and much of the computation time is wasted. By adapting the concept of envelope simulation, this computation expense can be saved.

The circuit envelope technique has been recently introduced in [4] and exploited in HP EEs of's ADS and MDS circuit design software. By discretizing and simulating the signal envelopes on the defined carrier, the envelope waveform has to be sampled faster than only the Nyquist rate of the signal envelope. This method has proven to be much more efficient than transient simulators like SPICE for narrow band cases. Y. Wang [5] adapted the same concept and developed a new transient electromagnetic solver called Envelope-Finite Element (EVFE) technique. The excitation and unknown fields are represented by a modulated format. The carrier signal is then de-embedded from the time-domain wave equation so that only the time-varying complex envelopes of the electromagnetic waves are simulated. Since only the signal envelope needs to be sampled, a much sparser time-step can be used than those in FDTD or FETD techniques, which results in much higher computation efficiency when the envelope/carrier ratio is small.

This paper extends the EVFE technique to three dimensions. As an example, a guided wave structure is analyzed to demonstrate the efficiency and the accuracy. This technique can be extended to incorporate with microwave lumped circuits by using the method introduced in [6].

II. THEORY

This section derives the formulation of the envelope-finite element (EVFE) technique in three dimensions. The

computational domain is terminated by 1st-order absorbing boundary conditions (ABC's). The general time-harmonic form of Maxwell's equations in a lossless region is

$$\nabla \times \nabla \times \left(\frac{\mathbf{E}}{\mu} \right) + \epsilon \frac{\partial^2 \mathbf{E}}{\partial t^2} + \frac{\partial \mathbf{J}}{\partial t} = 0 \quad (1)$$

where $\epsilon = \epsilon_r \epsilon_0$ and $\mu = \mu_r \mu_0$ are the permittivity and permeability, respectively. If the operational frequency bandwidth is narrow, then the first-order ABC's based on the traveling-wave assumption can be used to terminate the boundary. The ABC's used in FDTD or FETD can be expressed as

$$\nabla \times \mathbf{E} = -\hat{n} \times \frac{\sqrt{\epsilon_{\text{eff}}}}{c_0} \left(\frac{\partial \mathbf{E}}{\partial t} - 2 \frac{\partial \mathbf{E}^{\text{inc}}}{\partial t} \right) \text{ at the input port} \quad (2)$$

$$\nabla \times \mathbf{E} = -\hat{n} \times \frac{\sqrt{\epsilon_{\text{eff}}}}{c_0} \frac{\partial \mathbf{E}}{\partial t} \quad \text{at the output port} \quad (3)$$

where \hat{n} represents the surface normal of the boundary. By defining the carrier frequency ω_c , the field component and the current density can be written in a modulated signal format

$$\begin{aligned} \mathbf{E}(t) &= \mathbf{V}(t) e^{j\omega_c t} \\ \mathbf{J}(t) &= \mathbf{U}(t) e^{j\omega_c t} \end{aligned} \quad (4)$$

where $\mathbf{V}(t)$ and $\mathbf{U}(t)$ are the time-varying complex envelopes of the electric field and the excitation current at the carrier frequency, respectively. By substituting (4) into (1)-(3) and dividing both sides by $e^{j\omega_c t}$ yields the envelope equation

$$\begin{aligned} \nabla \times \nabla \times \left(\frac{\mathbf{V}}{\mu} \right) + \epsilon_0 \epsilon_r (-\omega_c^2 \mathbf{V} + 2j\omega_c \frac{\partial \mathbf{V}}{\partial t} + \frac{\partial^2 \mathbf{V}}{\partial t^2}) \\ = -(j\omega_c \mathbf{U} + \frac{\partial \mathbf{U}}{\partial t}) \end{aligned} \quad (5)$$

The ABC equations in EVFE simulation become

$$\nabla \times \mathbf{V} = -\hat{n} \times \frac{\sqrt{\epsilon_{\text{eff}}}}{c_0} \left[\left(\frac{\partial \mathbf{V}}{\partial t} + j\omega_c \mathbf{V} \right) - 2 \left(\frac{\partial \mathbf{V}^{\text{inc}}}{\partial t} + j\omega_c \mathbf{V}^{\text{inc}} \right) \right] \quad (6)$$

at the input port

$$\nabla \times \mathbf{V} = -\hat{n} \times \frac{\sqrt{\epsilon_{\text{eff}}}}{c_0} \left[\left(\frac{\partial \mathbf{V}}{\partial t} + j\omega_c \mathbf{V} \right) \right] \quad (7)$$

at the output port

The inner product of (5) with a testing function \mathbf{T} leads to the weak form shown in (8).

$$\begin{aligned} & \int \nabla \times \left(\frac{\mathbf{V}}{\mu} \right) \cdot \nabla \times \mathbf{T} dv + \int (-\epsilon \omega_c^2) \mathbf{T} \cdot \mathbf{V} dv + \\ & \int \left(\sqrt{\frac{\epsilon_0}{\mu_0}} \frac{\sqrt{\epsilon_{\text{eff}}}}{\mu_r} \right) (\hat{n} \times \mathbf{T}) \cdot [\hat{n} \times \left(\frac{\partial \mathbf{V}}{\partial t} + j\omega_c \mathbf{V} \right)] ds \\ & + \int (2j\omega_c \epsilon) \mathbf{T} \cdot \frac{\partial \mathbf{V}}{\partial t} dv + \int \epsilon \mathbf{T} \cdot \frac{\partial^2 \mathbf{V}}{\partial t^2} dv = \\ & \int_{\partial \Omega} \left(2 \sqrt{\frac{\epsilon_0}{\mu_0}} \frac{\sqrt{\epsilon_{\text{eff}}}}{\mu_r} \right) (\hat{n} \times \mathbf{T}) \cdot [\hat{n} \times \left(\frac{\partial \mathbf{V}^{\text{inc}}}{\partial t} + j\omega_c \mathbf{V}^{\text{inc}} \right)] ds \\ & + \int -\mathbf{T} \cdot (j\omega_c \mathbf{U} + \frac{\partial \mathbf{U}}{\partial t}) dv \end{aligned} \quad (8)$$

To solve (8) numerically, we discretize the space domain with tetrahedral elements and express the electric field in terms of basis functions associated with the edges of the elements as follows:

$$\mathbf{V} = \sum_{j=1}^N W_j^{(1)} \mathbf{v}_j, \mathbf{V}^{\text{inc}} = \sum_{j=1}^N W_j^{(1)} \mathbf{v}_j^{\text{inc}}, \mathbf{U} = \sum_{j=1}^N W_j^{(1)} \mathbf{j}_j \quad (9)$$

where N is the total number of the edges, $W_j^{(1)}$, a one-form Whitney element [7], is the vector basis function associated with edge j , and \mathbf{v}_j and \mathbf{j}_j are the circulations of the electric field and the current along the edge j , respectively. The application of Galerkin's process results in a system of ordinary differential equations

$$\begin{aligned} [\mathbf{G}_A] \underline{v} + [\mathbf{G}_B] \frac{\partial \underline{v}}{\partial t} + [\mathbf{G}_C] \frac{\partial^2 \underline{v}}{\partial t^2} &= [\mathbf{I}] (j\omega_c \underline{j} + \frac{\partial \underline{j}}{\partial t}) + \\ & [\mathbf{F}] \left(\frac{\partial \underline{v}^{\text{inc}}}{\partial t} + j\omega_c \underline{v}^{\text{inc}} \right) \end{aligned} \quad (10)$$

where \underline{v} , $\underline{v}^{\text{inc}}$, and \underline{j} are the vectors and $[\mathbf{G}_A]$, $[\mathbf{G}_B]$, $[\mathbf{G}_C]$, $[\mathbf{I}]$ and $[\mathbf{F}]$ are time-independent matrices. Those terms are given by

$$\begin{aligned} [\mathbf{G}_C]_{ij} &= \int (\epsilon_0 \epsilon_r) W_i^{(1)} \cdot W_j^{(1)} dv \\ [\mathbf{G}_D]_{ij} &= \int \left(\sqrt{\frac{\epsilon_0}{\mu_0}} \frac{\sqrt{\epsilon_r}}{\mu_r} \right) (\hat{n} \times W_i^{(1)}) \cdot (\hat{n} \times W_j^{(1)}) ds \\ [\mathbf{G}_A]_{ij} &= \int \frac{1}{\mu_0 \mu_r} \nabla \times W_i^{(1)} \cdot \nabla \times W_j^{(1)} dv - \omega_c^2 [\mathbf{G}_C]_{ij} + j\omega_c [\mathbf{G}_D]_{ij} \\ [\mathbf{G}_B]_{ij} &= 2j\omega_c [\mathbf{G}_C]_{ij} + j\omega_c [\mathbf{G}_D]_{ij} \\ [\mathbf{I}]_i &= \int -W_i^{(1)} \cdot dv \\ [\mathbf{F}]_i &= \int_{\partial \Omega} \left(2 \sqrt{\frac{\epsilon_0}{\mu_0}} \frac{\sqrt{\epsilon_r}}{\mu_r} \right) (\hat{n} \times W_i^{(1)}) \cdot (\hat{n} \times) ds \end{aligned}$$

The discretization in time domain is based on the Newmark-Beta formulation [8]

$$\begin{cases} \frac{d^2v}{dt^2} = \frac{1}{\Delta t^2} [v(n+1) - 2v(n) + v(n-1)] \\ \frac{dv}{dt} = \frac{1}{2\Delta t} [v(n+1) - v(n-1)] \\ v = \beta v(n+1) + (1-2\beta)v(n) + \beta v(n-1) \end{cases} \quad (11)$$

where $v(n) = v(n\Delta t)$ is the discrete-time representation of $v(t)$. Gedney [2] has proved that unconditional stability is achievable by choosing the interpolation parameter $\beta \geq 1/4$. This allows the time step to be chosen in order to give a specific accuracy without being constrained by the stability criteria. It was further shown that choosing $\beta = 1/4$ minimized solution error. Therefore, the resulting update scheme is

$$\begin{aligned} \left\{ \frac{[G_c]}{\Delta t^2} + \frac{[G_b]}{2\Delta t} + \frac{[G_a]}{4} \right\} v(n+1) &= \left\{ \frac{2[G_c]}{\Delta t^2} - \frac{[G_a]}{2} \right\} v(n) \\ + \left\{ -\frac{[G_c]}{\Delta t^2} + \frac{[G_b]}{2\Delta t} - \frac{[G_a]}{4} \right\} v(n-1) &+ [I] (j\omega_c j + \frac{\partial j}{\partial t}) \\ + [F] (\frac{\partial v^{inc}}{\partial t} + j\omega_c v^{inc}) \end{aligned} \quad (12)$$

To solve the system equations in (12), the matrix in the left-hand side needs to be inverted. Since this matrix is time-independent; it needs to be filled and solved only once if a direct sparse-matrix solver is used.

III. SIMULATION RESULT

A FORTRAN code based on the 3-D EVFE formulation given in Section II has been implemented and executed with an AMD 1.4 GHz PC machine. In this section, we compare numerical results between EVFE and unconditionally FETD techniques. The simulation structure is a rectangular waveguide with a dielectric post continuity shown in Fig. 1. The waveguide has a width $a = 22.86$ mm and height $b = 10.16$ mm. The dielectric slab has a height equal to that of the guide, a width $c = 12$ mm, and a length $d = 6$ mm. The dielectric constant of the slab is 8.2. The excitation of an electric probe consisting of a modulated Gaussian pulse is applied to excite a TE_{10} mode inside the waveguide; the carrier frequency is $f_c = 10$ GHz and half bandwidth is $\Delta f = 2.5$ GHz. The excitation in equation (8) is represented as

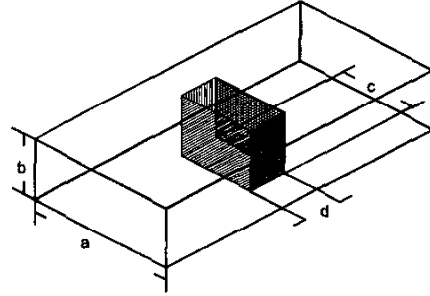


Fig. 1 Dielectric post discontinuity in a rectangular waveguide. $a = 22.86$ mm, $b = 10.16$ mm, $c = 12$ mm, $d = 6$ mm, and the dielectric constant of the slab $\epsilon_r = 8.2$. [9]

$$J(t) = U(t) e^{j\omega_c t} = \exp \left[\frac{(t-t_0)^2}{T^2} \right] \cdot e^{j\omega_c t} \quad (13)$$

where $T = 4/(\pi\Delta f)$, and $t_0 = 1.4T$.

The waveguide is terminated with first-order ABC's. The number of tetrahedrons in the finite element region is 72,373. A comparison of computation cost between the unconditionally stable FETD method and the EVFE method is listed in Table 1. The unknowns in FETD are real numbers, but complex numbers in EVFE. Thus, the matrix inversion in the latter method requires more time. The time steps are 5 ps in FETD and 25 ps in EVFE. Since two simulations have the same time duration, the total number of time steps is reduced from 1200 in unconditionally stable FETD to 240 in EVFE.

Table 1 Computation Times of the Structure in Fig. 1

	EVFE	FETD
Mesh Element Preprocessing	5 min.	3.5 min.
Matrix inversion	43 sec.	30 sec.
Time stepping	85 sec.	7 min.

Fig. 2 shows the magnitude of S_{11} and S_{21} in spectral domain for the structure shown in Fig. 1 using the unconditionally stable FETD method and the EVFE method. Fig. 3 shows the transient response of incident, reflected, and transmitted waves. The results show that the time step in EVFE method can be chosen to be five times

larger than that in the unconditionally stable FETD method to obtain the same quantitative accuracy.

IV. CONCLUSION

The 3-D Envelope-Finite Element Technique (EVFE) has been implemented and applied to solve a guided wave structure. The time step size used in unconditionally stable FETD can be more than ten times that of the conventional FETD. This paper has shown that EVFE can improve the computation efficiency of unconditionally stable FETD by a factor of the carrier-to-envelop frequency ratio. For high

frequency, narrowband EM analysis, this method becomes the best candidate for cost-effective full-time simulation.

REFERENCES

- [1] X. Zhang, J. Fang, K. K. Mei, and Y. Liu, "Calculations of the dispersive characteristics of microstrips by the time-domain finite difference method," *IEEE Trans. Microwave Theory and Tech.*, vol. MTT-36, no. 2, pp.263-267, Feb. 1988.
- [2] A. D. Gedney, and U. Navsariwala, "An Unconditionally Stable Finite Element Time-Domain Solution of the Vector Wave Equation," *IEEE Microwave and Guided Wave Letters*, vol.5, (no.10), pp.332-334, Oct. 1995.
- [3] H-P Tsai, Y. Wang, and T. Itoh, "An Unconditionally Stable Extended (USE) Finite Element Time Domain Solution of Active Nonlinear Microwave Circuits Using Perfectly Matched Layers," accepted for publication in *IEEE Trans. Microwave Theory Tech.*.
- [4] H. S. Yap, "Designing to digital wireless specifications using circuit envelope simulation," *1997 Asia Pacific Microwave Conference*, pp.173-176.
- [5] Y. Wang and T. Itoh, "Envelope-Finite Element (EVFE) Technique - A More Efficient Time Domain Scheme," *IEEE Trans. Microwave Theory and Tech.*, vol. 49 , no. 12, pp., Dec. 2001.
- [6] S.-H. Chang, R. Cocciali, Y. Qian, and T. Itoh, "A Global Finite-Element Time Domain Analysis of Active Nonlinear Microwave," *IEEE Trans. Microwave Theory Tech.*, vol.47, (no.12), pp.2410-16, Dec. 1999.
- [7] A. Bossavit, "Whitney form: A class of finite elements for three-dimensional computations in electromagnetism," *Proc. Inst. Elect. Eng.*, vol. 135, pt. A, no. 8, pp. 493-500, Nov. 1988.
- [8] N. M. Newmark, "A method of computation for structural dynamics," *J. Engineering Mechanics Division, ASCE*, vol. 85, pp. 67-94, July 1959.
- [9] J-S Wang and R. Mittra, "Finite Element Analysis of MMIC Structures and Electronic Packages Using Absorbing Boundary Conditions," *IEEE Trans. Microwave Theory and Tech.*, vol. 42, no. 3, pp. 441-449, Mar. 1994.

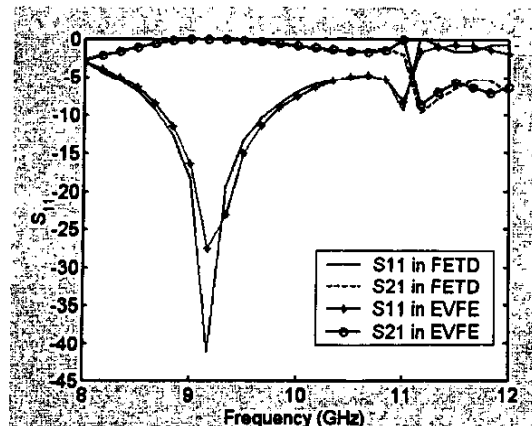


Fig.2. Reflection coefficient of the transition rectangular waveguide to dielectric slab loaded waveguide.

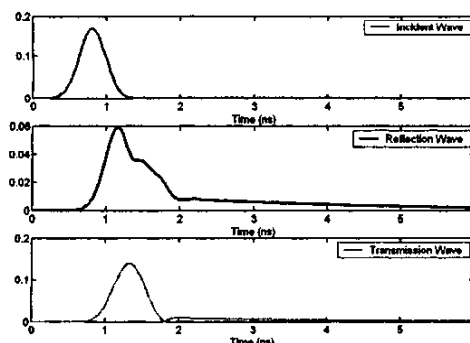


Fig. 3 The transient signal envelope of the dielectric post discontinuity in a rectangular waveguide.